

Lone-Pair Activity in Lead(II) Complexes with Unsymmetrical Lariat Ethers

David Esteban-Gómez, Carlos Platas-Iglesias, Teresa Enríquez-Pérez, Fernando Avecilla, Andrés de Blas,* and Teresa Rodríguez-Blas*

Departamento de Química Fundamental, Universidade da Coruña, Campus da Zapateira, s/n 15071 A Coruña, Spain

Received February 14, 2006

We have carried out a study about the structural effect of the lone-pair activity in lead(II) complexes with the unsymmetrical lariat ethers L^7 , L^8 , $(L^8-H)^-$, $(L^9-H)^-$, and $(L^{10}-H)^-$. All these ligands are octadentate and differ by the aromatic unit present in their backbones: pyridine, phenol, phenolate, thiophenolate, and pyrrolate, respectively. In these lead(II) complexes, the receptor may adopt two possible syn conformations, depending on the disposition of the pendant arms over the crown moiety fragment. The conformation where the pendant arm holding the imine group is placed above the macrocyclic chain containing two ether oxygen atoms has been denoted as I, whereas the term II refers to the conformation in which such pendant arm is placed above the macrocyclic chain containing the single oxygen atom. Compounds of formula $[Pb(L^7)](ClO_4)_2$ (**1**) and $[Pb(L^8-H)](ClO_4)$ (**2**) were isolated and structurally characterized by X-ray diffraction analyses. The crystal structure of **1** adopts conformation I and shows the lead(II) ion bound to the eight available donor atoms of the bibracchial lariat ether in a holodirected geometry, whereas the geometry of **2** is best described as hemidirected, with the receptor adopting conformation II. The five systems $[Pb(L^7)]^{2+}$, $[Pb(L^8)]^{2+}$, $[Pb(L^8-H)]^+$, $[Pb(L^9-H)]^+$, and $[Pb(L^{10}-H)]^+$ were characterized by means of density functional theory calculations (DFT) performed by using the B3LYP model. An analysis of the natural bond orbitals (NBOs) indicates that the Pb(II) lone-pair orbital remains almost entirely s in character in the $[Pb(L^7)]^{2+}$ complexes, whereas in $[Pb(L^8-H)]^+$, the Pb(II) lone pair is polarized by a certain 6p contribution. The reasons for the different roles of the Pb(II) lone pair in compounds **1** and **2** as well as in the related model compounds are discussed. Our results point to the presence of a charged donor atom in the ligand (such as a phenolate oxygen atom, pyrrolate nitrogen atom, or even thiophenolate sulfur atom) favoring hemidirected geometries.

Introduction

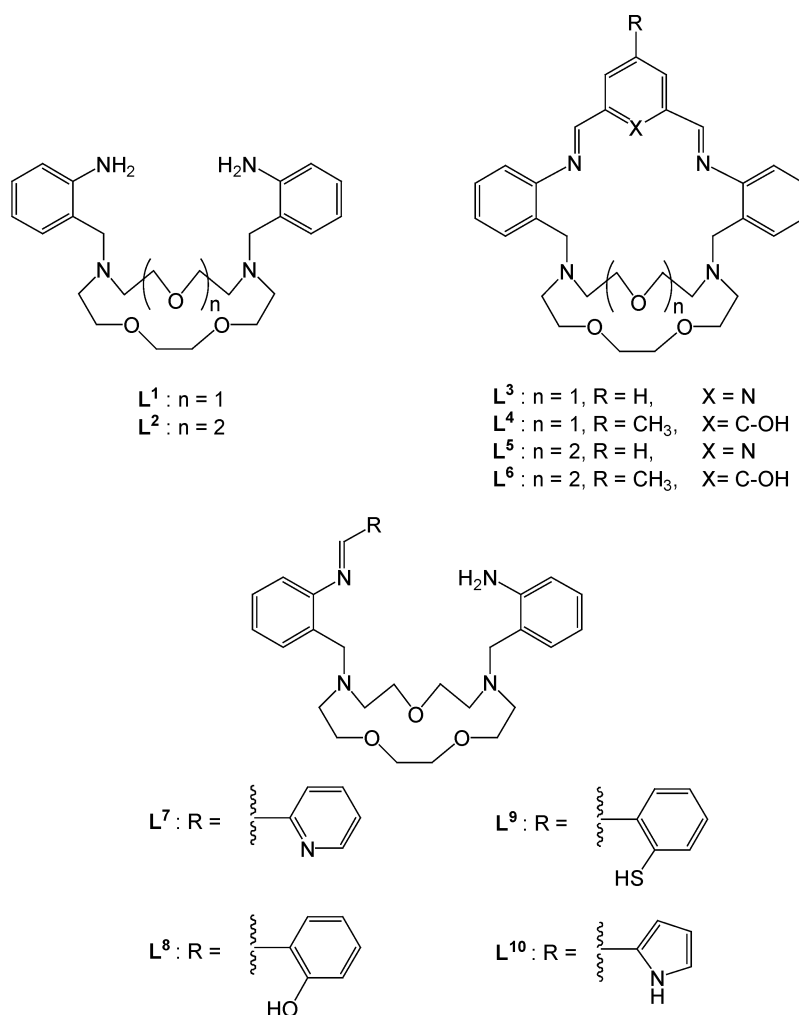
The concept of a chemically inert but stereochemically active $6s^2$ lone pair is commonly associated with Pb(II) and other post-transition metal ions, such as Sn(II) and Bi(III). Several authors have studied structural effects caused by the Pb(II) lone pair both in solid-state materials¹ and coordination compounds.^{2–4} In particular, Shimoni-Livny et al.⁵ investi-

gated a close relation between the role of a lone pair of Pb(II) and the coordination geometry for a large number of Pb(II) complexes. They have found two general structural categories of Pb(II) compounds, holodirected and hemidirected, which are distinguished by the disposition of ligands around the metal ion. There so, in the hemidirected form, there is a void in the liganding that is not found in holodirected geometry. Complexes with high coordination numbers (9–10) usually adopt a holodirected geometry, whereas lead(II) complexes with coordination numbers less than 6 are normally hemidirected and have a stereochemically active lone pair. Both types of structures are found for intermediate coordination numbers (6–8). In this case, the stereochemical activity of the lone pair, and hence the geometry, seems to strongly depend on the nature of the donor atoms and the steric repulsion of the ligands. It has been stated that for electro-negative donor atoms such as oxygen or nitrogen, hemidirected structures are energetically favored. Likewise, mo-

* To whom correspondence should be addressed. E-mail: mayter@udc.es (T.R.-B.). Tel: 34-981-16-70-00 ext. 2132. Fax: 34-981-16-70-65.

- (1) Walsh, A.; Watson, G. W. *J. Solid State Chem.* **2005**, *178*, 1422–1428.
- (2) Hancock, R. D.; Reibenspies, J. H.; Maumela, H. *Inorg. Chem.* **2004**, *43*, 2981–2987.
- (3) Hancock, R. D.; Shaikjee, M. S.; Dobson, S. M.; Boeyens, J. C. *Inorg. Chim. Acta* **1988**, *154*, 229.
- (4) Luckay, R.; Cukrowski, I.; Mashishi, J.; Reibenspies, J. H.; Bond, A. H.; Rogers, R. D.; Hancock, R. D. *J. Chem. Soc., Dalton Trans.* **1997**, 901.
- (5) Shimoni-Livny, L.; Glusker, J. P.; Bock, C. W. *Inorg. Chem.* **1998**, *37*, 1853.

Chart 1



lecular-orbital calculations suggest that repulsive interactions between very polarizable ligands as a result of their effective charge may result in holodirected structures.⁶

The majority of those studies concerning the Pb(II) lone-pair activity have been carried out using ligands with low denticity. However, similar studies on complexes with ligands of high denticity (greater than five) are scarce. In the latter case, the dependence between the stereochemical activity of the Pb(II) lone pair and the nature of the donor atoms is not so clear. As a part of our research project, we are interested in assessing the lone-pair activity in lead(II) complexes containing polydentate ligands derived from crown ethers. To date, we have reported studies with the ligands L^1 – L^6 shown in Chart 1.^{7–9} L^1 and L^2 are symmetrical bibrachial lariet ethers, whereas L^3 – L^6 are related Schiff-base lateral macrobicycles. As a continuation of these works, in the present paper, we study the structural effect of the Pb(II) $6s^2$ lone pair in the corresponding complexes with the unsymmetrical lariet ethers L^7 – L^{10} , which are structurally derived from L^1 .

The X-ray crystal structures of the lead(II) complexes with receptors L^7 and the deprotonated form of L^8 , $[Pb(L^7)]-$

$(ClO_4)_2$ (**1**) and $[Pb(L^8-H)](ClO_4)$ (**2**), are reported. To understand the structural features and electronic properties of these systems related to the stereochemical activity of the lead(II) lone pair, as well as those of their analogues with L^9 and L^{10} , we turned to theory. The accurate calculation of the electronic structure of metal complexes remains a challenging task for quantum chemistry. Although both Hartree–Fock and DFT calculations have been used for this purpose, the latter has certain advantages over the former.¹⁰ In the DFT method, correlation is partly taken into account by considering the functional form of the exchange–correlation contribution. Thus, DFT appears to be an excellent approach for optimizing the geometries and exploring the electronic structure of metal complexes, including Pb(II) coordination compounds.¹¹ Thus, we also report electronic structure calculations on the basis of density functional theory

(7) Esteban, D.; Bañobre, D.; de Blas, A.; Rodríguez-Blas, T.; Bastida, R.; Macías, A.; Rodríguez, A.; Fenton, D. E.; Adams, H.; Mahía, J. *Eur. J. Inorg. Chem.* **2000**, 1445.

(8) Esteban, D.; Avecilla, F.; Platas-Iglesias, C.; Mahía, J.; de Blas, A.; Rodríguez-Blas, T. *Inorg. Chem.* **2002**, *41*, 4337.

(9) Esteban-Gomez, D.; Ferreirós, R.; Fernandez-Martinez, S.; Avecilla, F.; Platas-Iglesias, C.; de Blas, A.; Rodriguez-Blas, T. *Inorg. Chem.* **2005**, *44*, 5428.

(10) Foresman, J. B.; Frisch, A. E. *Exploring Chemistry with Electronic Structure Methods*, 2nd ed.; Gaussian Inc.: Pittsburgh, PA, 1996; Chapter 6.

(6) Claudio, E. S.; Godwin, H. A.; Magyar, J. S. *Prog. Inorg. Chem.* **2003**, *51*, 1.

(DFT) on the $[\text{Pb}(\text{L}^7)]^{2+}$, $[\text{Pb}(\text{L}^8)]^{2+}$, $[\text{Pb}(\text{L}^8\text{-H})]^+$, $[\text{Pb}(\text{L}^9\text{-H})]^+$ and $[\text{Pb}(\text{L}^{10}\text{-H})]^+$ systems, which allows us to rationalize the stereochemical activity of the lead(II) lone pair in these kinds of compounds.

Experimental Section

General Considerations. *N,N'*-Bis(2-aminobenzyl)-1,10-diaza-15-crown-5 (**L**¹) was prepared as previously described.⁷ All other chemicals were purchased from commercial sources and used without further purification. Solvents were of reagent grade purified by the usual methods. **Caution!** *Although we have experienced no difficulties with the perchlorate salts, these should be regarded as potentially explosive and handled with care.*¹²

Elemental analyses were carried out on a Carlo Erba 1180 elemental analyzer, and FAB-MS were recorded on a FISONS QUATRO mass spectrometer with a Cs ion gun using 3-nitrobenzyl alcohol as the matrix. ¹H and ¹³C NMR spectra were run on a Bruker Avance 300 MHz spectrometer. IR spectra were recorded as KBr disks, using a Bruker Vector 22 spectrophotometer. Conductivity measurements were carried out at 20 °C with a Crison Micro CM 2201 conductivitymeter using 1×10^{-3} M solutions of the complexes in acetonitrile.

Preparation of the Complexes. $[\text{Pb}(\text{L}^7)](\text{ClO}_4)_2$ (1**).** A solution of *N,N'*-bis(2-aminobenzyl)-1,10-diaza-15-crown-5 (0.065 g, 0.15 mmol) and 2-formylpyridine (0.016 g, 0.15 mmol) in absolute ethanol (50 mL) was stirred and refluxed for 48 h. A solution of $\text{Pb}(\text{ClO}_4)_2 \cdot 3\text{H}_2\text{O}$ (0.070 g, 0.15 mmol) in absolute ethanol (10 mL) was added to the former solution, and the mixture was stirred and refluxed for 24 h. The resulting deep yellow solution was filtered while hot; the filtrate was concentrated to 25 mL, giving a yellow precipitate that was isolated by filtration and air-dried (yield: 0.098 g, 67%). Anal. Calcd for $\text{C}_{30}\text{H}_{39}\text{Cl}_2\text{N}_5\text{O}_{11}\text{Pb} \cdot \text{EtOH}$: C, 39.6; H, 4.7; N, 7.2. Found: C, 40.3; H, 4.4; N, 7.3. FAB-MS (*m/z* (%BPI)): 824 (100) $[\text{Pb}(\text{L}^7)(\text{ClO}_4)]^+$. IR (KBr): 3362 $\nu_{\text{as}}(\text{NH}_2)$, 3298 $\nu_{\text{s}}(\text{NH}_2)$, 1627 $\nu(\text{C}=\text{N})_{\text{imine}}$, 1092 $\nu_{\text{as}}(\text{Cl}-\text{O})$, 623 $\delta_{\text{as}}(\text{O}-\text{Cl}-\text{O})$ cm^{-1} . X-ray quality crystals of **1** were grown by slow diffusion of diethyl ether into a solution of the complex in acetonitrile.

$[\text{Pb}(\text{L}^8\text{-H})](\text{ClO}_4)$ (2**).** A solution of *N,N'*-bis(2-aminobenzyl)-1,10-diaza-15-crown-5 (0.080 g, 0.20 mmol) and salicylaldehyde (0.023 g, 0.20 mmol) in absolute ethanol (50 mL) was stirred and refluxed for 24 h. Triethylamine (0.038 g, 0.40 mmol) was added, and the resulting solution was stirred and refluxed for 24 h. A solution of $\text{Pb}(\text{ClO}_4)_2 \cdot 3\text{H}_2\text{O}$ (0.086 g, 0.20 mmol) in absolute ethanol (10 mL) was added to the former solution, and the mixture was stirred and refluxed for 36 h. The resulting deep yellow solution was filtered while hot; the filtrate was concentrated to 25 mL, giving a yellow precipitate that was isolated by filtration and air-dried (yield: 0.047 g, 30%). Anal. Calcd for $\text{C}_{31}\text{H}_{39}\text{ClN}_4\text{O}_5\text{Pb}$: C, 47.1; H, 5.0; N, 7.1. Found: C, 47.3; H, 5.0; N, 7.0. FAB-MS (*m/z* (%BPI)): 739 (100) $[\text{Pb}(\text{L}^8\text{-H})]^+$. IR (KBr): 3350 $\nu_{\text{as}}(\text{NH}_2)$, 3289 $\nu_{\text{s}}(\text{NH}_2)$, 1613 $\nu(\text{C}=\text{N})_{\text{imine}}$, 1093 $\nu_{\text{as}}(\text{Cl}-\text{O})$, 623 $\delta_{\text{as}}(\text{O}-\text{Cl}-\text{O})$ cm^{-1} . X-ray quality crystals of **2** were grown by slow diffusion of diethyl ether into a solution of the complex in methanol.

Crystal Structure Determinations. Crystal data and details on data collection and refinement are summarized in Table 1. Three-dimensional X-ray data were collected in the θ range 1.83–28.34° (**1**) and 1.87–28.30° (**2**) on a Bruker Smart 1000 CCD instrument. Reflections were measured from a hemisphere of data collected

Table 1. Crystal Data and Structure Refinement for **1** and **2**

	1	2
formula	$\text{C}_{30}\text{H}_{39}\text{Cl}_2\text{N}_5\text{O}_{11}\text{Pb}$	$\text{C}_{31}\text{H}_{39}\text{ClN}_4\text{O}_8\text{Pb}$
mol wt	923.76	838.30
space group	$P2_1/n$	$P2_12_12_1$
cryst syst	monoclinic	orthorhombic
<i>a</i> (Å)	9.2846(7)	13.7050(18)
<i>b</i> (Å)	11.8696(9)	14.721(2)
<i>c</i> (Å)	31.908(2)	16.220(2)
β (deg)	93.228(2)	90
<i>V</i> (Å ³)	3510.8(5)	3272.4(7)
<i>Z</i>	4	4
<i>T</i> (K)	298(2)	298(2)
$\lambda(\text{Mo K}\alpha)$ (Å)	0.71073	0.71073
<i>D</i> _{calcd} (g cm ⁻³)	1.748	1.702
μ (mm ⁻¹)	5.022	5.292
<i>R</i> _{int}	0.0977	0.1490
no. of reflns measd	24 425	20 723
no. of reflns obsd	3799	3042
<i>R</i> ₁ ^a	0.0510	0.0613
w <i>R</i> ₂ (all data) ^b	0.0955	0.1387

$$^a R_1 = \sum |F_o| - |F_c| / \sum |F_o|. \quad ^b wR_2 = \{ \sum [w(|F_o|^2 - |F_c|^2)^2] / \sum [w(F_o^4)] \}^{1/2}.$$

from frames, each covering 0.3° in ω . Of the 24 425 (**1**) and 20 723 (**2**) reflections measured, all of which were corrected for Lorentz and polarization effects and for absorption by semiempirical methods on the basis of symmetry-equivalent and repeated reflections, 3799 (**1**) and 3042 (**2**) independent reflections exceeded the significance level ($|F|/(\sigma|F|)) > 4.0$. The structures were solved by direct methods and refined by full matrix least-squares on F^2 . Hydrogen atoms were included in calculated positions and refined in the riding mode. Refinement was performed with allowance for thermal anisotropy of all non-hydrogen atoms. Minimum and maximum final electronic densities were -0.963 and $1.077 \text{ e } \text{Å}^{-3}$ for **1** and -1.579 and $0.936 \text{ e } \text{Å}^{-3}$ for **2**. Complex scattering factors were taken from the program package SHELXTL,¹³ as implemented on a Pentium computer.

Computational Methods. The $[\text{Pb}(\text{L}^7)]^{2+}$, $[\text{Pb}(\text{L}^8)]^{2+}$, $[\text{Pb}(\text{L}^8\text{-H})]^+$, $[\text{Pb}(\text{L}^9\text{-H})]^+$ and $[\text{Pb}(\text{L}^{10}\text{-H})]^+$ systems were fully optimized by using the B3LYP density functional model.^{14,15} In these calculations, we have used the standard 6-31G* basis set for the ligand atoms, whereas the LanL2DZ valence and effective core potential functions were used for Pb.^{16,17} X-ray structures were used as input geometries when available. The stationary points found on the potential energy surfaces as a result of the geometry optimizations of the complexes have been tested to represent energy minima rather than saddle points via frequency analysis. The in vacuo relative energies of conformation II with respect to conformation I were calculated including non-potential-energy contributions (that is, zero-point energy and thermal terms) obtained by frequency analysis. Single-point energies were calculated in acetonitrile solution on the optimized structures by using the 6-31G* and 6-311G** basis sets for the ligand atoms. Solvent effects were included by using the Klamt's form of the conductor reaction field (COSMO).¹⁸ The solute cavity is built as an envelope of spheres centered on atoms or atomic groups with appropriate radii. Each sphere is subdivided into 60 initial tesserae in pentakis-dodecahedral

(11) Platas-Iglesias, C.; Esteban-Gómez, D.; Enríquez-Pérez, T.; Avecilla, F.; De Blas, A.; Rodríguez-Blas, T. *Inorg. Chem.* **2005**, *44*, 2224–2233.

(12) Wolsey, W. C. *J. Chem. Educ.* **1973**, *50*, A335.

(13) Sheldrick, G. M. *SHELXTL*, release 5.1; Bruker Analytical X-ray System: Madison, WI, 1997.

(14) Becke, A. D. *J. Chem. Phys.* **1993**, *98*, 5648.

(15) Lee, C.; Yang, W.; Parr, R. G. *Phys. Rev. B* **1988**, *37*, 785.

(16) Hay, P. J.; Wadt, W. R. *J. Chem. Phys.* **1985**, *82*, 270.

(17) A description of the basis sets and theory level used in this work can be found in: Foresman, J. B.; Frisch, A. E. *Exploring Chemistry with Electronic Structure Methods*, 2nd ed.; Gaussian Inc.: Pittsburgh, PA, 1996.

(18) Eckert, F.; Klamt, A. *AICHe J.* **2002**, *48*, 369.

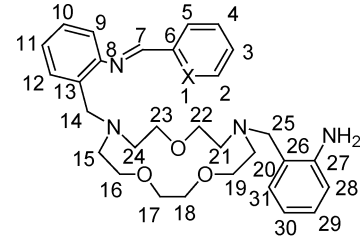
patterns. The wave functions of some of the lead complexes were analyzed by natural bond orbital analyses, involving natural atomic orbital (NAO) populations and natural bond orbitals (NBO).^{19,20} The NMR shielding tensors of the $[\text{Pb}(\text{L}^8\text{-H})]^+$ system were calculated in acetonitrile solution by using the GIAO method.²¹ In these calculations, we have used the LanL2DZ valence and effective core potential functions for Pb, and the 6-311G** basis set on ligand atoms. For ^{13}C NMR chemical shift calculation purposes, tetramethylsilane (TMS) was optimized in vacuo at the B3LYP/6-31G* computational level. On the optimized structure, the ^{13}C NMR shielding tensors of TMS were calculated in acetonitrile solution (COSMO model) by using the 6-311G** basis set. All DFT calculations were performed by using the Gaussian 03 program package (revision C.01).²²

Results and Discussion

Synthesis and Characterization of (1) and (2). Compounds of formula $[\text{Pb}(\text{L}^7)](\text{ClO}_4)_2$ (**1**) and $[\text{Pb}(\text{L}^8\text{-H})](\text{ClO}_4)$ (**2**) can be easily prepared by a conventional Schiff-base condensation between the bibracchial lariat ether *N,N'*-bis(2-aminobenzyl)-1,10-diaza-15-crown-5 (**L**¹) and 2-formylpyridine or salicylaldehyde and subsequent reaction with hydrated lead(II) perchlorate. To deprotonate the phenolic group of **L**⁸, we added 1 equiv of triethylamine to the reaction mixture. The IR spectra of both **1** and **2** (KBr disks) show two bands at ca. 3350 cm^{-1} and another two at ca. 3300 cm^{-1} , corresponding to the $\nu_{\text{as}}(\text{NH}_2)$ and $\nu_{\text{s}}(\text{NH}_2)$ stretching modes of the coordinated amine groups, respectively. Moreover, the spectra also show a band at 1627 (**1**) or 1613 (**2**) cm^{-1} that is attributable to the $\nu(\text{C}=\text{N})$ stretching mode of the imine group. Bands corresponding to the $\nu_{\text{as}}(\text{ClO})$ stretching and $\delta_{\text{as}}(\text{OClO})$ bending modes of the perchlorate groups present in **1** and **2** appear without splitting at ca. 1090 and 624 cm^{-1} , respectively, as befits an uncoordinated anion. The FAB-mass spectra of these complexes display peaks due to $[\text{Pb}(\text{L}^7)(\text{ClO}_4)]^+$ (**1**) and $[\text{Pb}(\text{L}^8\text{-H})]^+$ (**2**) at m/z (%BPI) = 824 (100) and 739 (100), respectively. These results confirm that condensation has occurred only in one pendant arm of **L**¹ and that the lead(II) complexes with the corresponding unsymmetrical ligand have been formed.

The ^1H and ^{13}C NMR spectra of compound **1** were recorded in acetonitrile- d_3 solution at 298 K and assigned

Table 2. ^1H and ^{13}C NMR Shifts (δ , ppm with respect to TMS) for Compounds **1** and **2**^a



L⁷: X = N
L⁸: X = C-OH

1			2				
	^1H	^{13}C		^1H	^{13}C		
H2	8.20 (m, 3H)	C2	151.4	H2	6.59 (m, 2H)	C1	169.4
H3	7.57 (td, 1H)	C3	129.8	H3	7.45 (m, 2H)	C2	125.6
H4	8.20 (m, 3H)	C4	141.5	H4	6.59 (m, 2H)	C3	136.8
H5	8.2 (m, 3H)	C5	132.1	H5	7.45 (m, 2H)	C4	115.9
H7	9.35 (s, 1H)	C6	153.4	H7	8.43 (s, 1H)	C5	138.0
H9	7.53 (d, 1H)	C7	167.7	H9	7.32 (m, 3H)	C6	125.3
H10	7.68 (m, 1H)	C8	149.1	H10	7.56 (t, 1H)	C7	168.2
H11	7.48 (m, 2H)	C9	122.6	H11	7.32 (m, 3H)	C8	152.3
H12	7.48 (m, 2H)	C10	132.5	H12	7.32 (m, 3H)	C9	124.1
H14a	3.54 (d, 1H)	C11	130.0	H28	6.50 (d, 1H)	C10	130.6
H14b	4.60 (d, 1H)	C12	135.3	H29	7.12 (m, 2H)	C11	127.8
H15ax	2.61 (m)	C13	130.5	H30	6.83 (t, 1H)	C12	134.0
H15eq	3.02 (m)	C14	57.6	H31	7.12 (m, 2H)	C13	131.8
H16ax	3.74 (m)	C15	54.5	H14–H25	2.4–4.2 (m, 24H)	C14	59.9
H16eq	4.10 (m)	C16	69.2	NH ₂	4.19 (s, 2H)	C15	56.8
H17ax	3.59 (m)	C17	70.4			C16	69.5
H17eq	3.71 (m)	C18	70.8			C17	70.4
H18ax	3.59 (m)	C19	69.1			C18	70.2
H18eq	3.75 (m)	C20	54.0			C19	69.5
H19ax	3.75 (m)	C21	54.7			C20	55.1
H19eq	4.16 (m)	C22	69.6			C21	56.0
H20ax	2.59 (m)	C23	68.8			C22	69.3
H20eq	3.10 (m)	C24	54.0			C23	69.9
H21ax	2.68 (m)	C25	56.5			C24	56.4
H21eq	3.43 (m)	C26	125.7			C25	59.6
H22ax	3.83 (m)	C27	142.1			C26	126.2
H22eq	4.18 (m)	C28	120.9			C27	143.5
H23ax	3.79 (m)	C29	130.9			C28	120.9
H23eq	3.89 (m)	C30	123.7			C29	122.7
H24ax	2.54 (m)	C31	134.5			C30	
H24eq	2.97 (m)					C31	134.2
H25a	3.39 (d, 1H)						
H25b	4.03 (d, 1H)						
H28	6.23 (dd, 1H)						
H29	6.81 (m, 2H)						
H30	6.81 (m, 2H)						
H31	7.15 (dd, 1H)						
NH ₂	4.21 (s, 2H)						

^a Conditions: T = 298 K, CD₃CN, 300 MHz. $J_{16,15} = J_{15,16} = 7.81$ Hz. Assignment supported by 2D H,H COSY, HSQC, and HMBC experiments.

on the basis of two-dimensional COSY, HSQC, and HMBC experiments. The ^1H NMR spectrum is shown in Figure S1 of the Supporting Information, and the results are summarized in Table 2. Because assignments to specific axial/equatorial CH₂ protons were not possible on the basis of the 2D NMR spectra, they were carried out using the stereochemically dependent proton shift effects, resulting from the polarization of the C–H bonds by the electric field generated by the cation charge,²³ as predicted from the X-ray crystal structure of **1**. This polarization results in a deshield-

- (19) Glendening, E. D.; Reed, A. E.; Carpenter, J. E.; Weinhold, F. *NBO*, version 3.1; Gaussian Inc.: Pittsburgh, PA, 1992.
- (20) Reed, A. E.; Curtiss, L. A.; Weinhold, F. *Chem. Rev.* **1988**, *88*, 899.
- (21) Ditchfield, R. *Mol. Phys.* **1974**, *27*, 789.
- (22) Frisch, M. J.; Trucks, G. W.; Schlegel, H. B.; Scuseria, G. E.; Robb, M. A.; Cheeseman, J. R.; Montgomery, J. A., Jr.; Vreven, T.; Kudin, K. N.; Burant, J. C.; Millam, J. M.; Iyengar, S. S.; Tomasi, J.; Barone, V.; Mennucci, B.; Cossi, M.; Scalmani, G.; Rega, N.; Petersson, G. A.; Nakatsuji, H.; Hada, M.; Ehara, M.; Toyota, K.; Fukuda, R.; Hasegawa, J.; Ishida, M.; Nakajima, T.; Honda, Y.; Kitao, O.; Nakai, H.; Klene, M.; Li, X.; Knox, J. E.; Hratchian, H. P.; Cross, J. B.; Bakken, V.; Adamo, C.; Jaramillo, J.; Gomperts, R.; Stratmann, R. E.; Yazyev, O.; Austin, A. J.; Cammi, R.; Pomelli, C.; Ochterski, J. W.; Ayala, P. Y.; Morokuma, K.; Voth, G. A.; Salvador, P.; Dannenberg, J. J.; Zakrzewski, V. G.; Dapprich, S.; Daniels, A. D.; Strain, M. C.; Farkas, O.; Malick, D. K.; Rabuck, A. D.; Raghavachari, K.; Foresman, J. B.; Ortiz, J. V.; Cui, Q.; Baboul, A. G.; Clifford, S.; Cioslowski, J.; Stefanov, B. B.; Liu, G.; Liashenko, A.; Piskorz, P.; Komaromi, I.; Martin, R. L.; Fox, D. J.; Keith, T.; Al-Laham, M. A.; Peng, C. Y.; Nanayakkara, A.; Challacombe, M.; Gill, P. M. W.; Johnson, B.; Chen, W.; Wong, M. W.; Gonzalez, C.; Pople, J. A. *Gaussian03*, revision C.01; Gaussian Inc.: Wallingford, CT, 2004.

- (23) Gonzalez-Lorenzo, M.; Platas-Iglesias, C.; Vecilla, F.; Galdes, C. F. G. C.; Imbert, D.; Bünzli, J.-C. G.; de Blas, A.; Rodríguez-Blas, T. *Inorg. Chem.* **2003**, *42*, 6946.

ing of the equatorial protons, which are pointing away from the metal ion. The H14 methylene protons show an AB pattern ($^2J_{14a-14b} = 12.1$ Hz) in which the protons labeled as b are again deshielded because they are pointing away from the metal ion. A similar situation occurs for the H25 methylene protons ($^2J_{25a-25b} = 13.3$ Hz).

The ^1H NMR spectrum of **2** displays relatively broad resonances for several proton signals occurring in the aliphatic region (Figure S1 of the Supporting Information), which prevented the observation of many expected cross-peaks in the two-dimensional HMBC experiments. A full assignment of the ^{13}C NMR spectrum (Table 2) was achieved with the aid of theoretical calculations by using the GIAO method,²¹ which has been shown to be a useful tool for the prediction of ^{13}C NMR spectra of complexes with lariat ethers.²⁴ Calculated ^{13}C NMR shifts are compared to the experimental ones in Table S1 of the Supporting Information. The ^1H NMR spectra of **1** and **2** display a remarkable difference in the signal due to the imine protons, which appears as a singlet in both spectra; however, the signal is flanked by satellites attributable to proton coupling with the naturally abundant ^{207}Pb ($I = 1/2$),²⁵ with $^3J(^1\text{H}-^{207}\text{Pb}) = 13.4$ Hz, in the spectrum of **2**. This coupling reflects kinetic inertness in the complex, as well as a degree of covalence in the interaction between the lead(II) ion and the nearby donor atom.

X-ray Crystal Structures of (1) and (2) and DFT Optimized Geometries. Slow diffusion of diethyl ether into solutions of compounds **1** and **2** in acetonitrile or methanol, respectively, gave yellow single crystals suitable for X-ray diffraction. Crystals contain the cations $[\text{Pb}(\text{L}^7)]^{2+}$ (**1**) and $[\text{Pb}(\text{L}^8-\text{H})]^+$ (**2**) and perchlorate anions involved in hydrogen-bonding interactions. Figure 1 shows a view of both complex cations, whereas bond lengths of the metal-coordination environment are listed in Table 3. Bond angles of the metal-coordination sphere are given in Table S2 of the Supporting Information. In both $[\text{Pb}(\text{L}^7)]^{2+}$ and $[\text{Pb}(\text{L}^8-\text{H})]^+$, the lead(II) ion is placed over the plane of the macrocyclic ring, resulting in a syn conformation with the sidearms orientated on the same side of the crown moiety. Likewise, the lone pairs of both pivotal nitrogen atoms are forced to point toward the receptor cavity in an endo–endo conformation. It must be remarked that the syn conformation adopted by the lariat ether confers to the complex a chiral structure with two possible optical isomers that can be labeled as Δ or Λ .²⁶ Indeed, compound **2** crystallizes in the chiral $P2_12_12_1$ orthorhombic space group, and only one enantiomer is found in the crystal. However, it is surprising that despite its chirality, compound **1** crystallizes in the $P2_1/n$ space group,

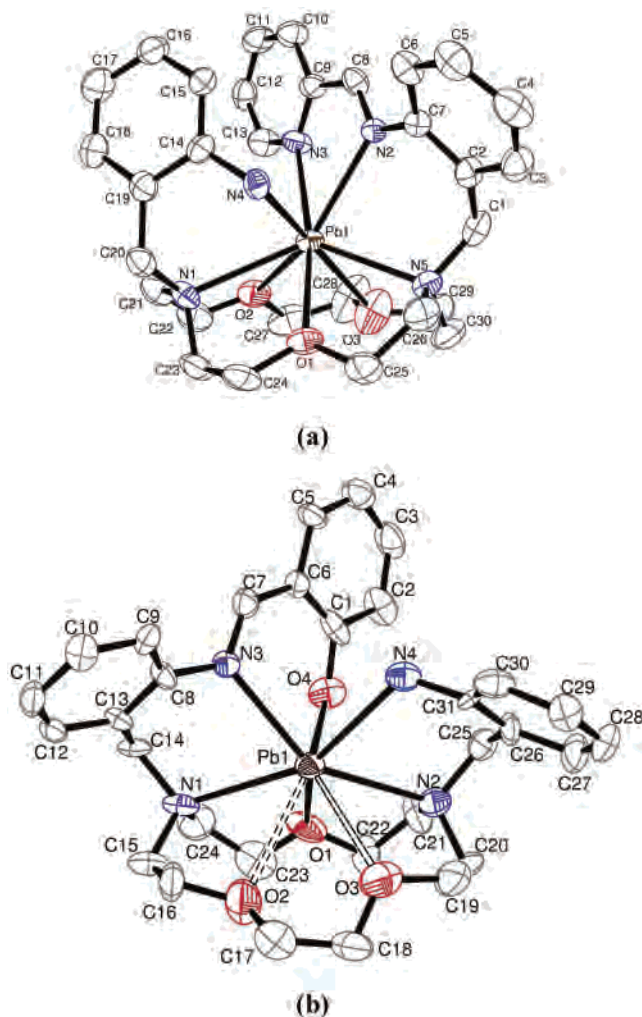


Figure 1. X-ray crystal structures of the cations in (a) compound **1** and (b) compound **2**, with atom labeling; hydrogen atoms are omitted for simplicity. The ORTEP plot is drawn at the 33% probability level.

which is not chiral. This is because the crystal contains a racemic mixture of both enantiomers centrosymmetrically related.

In $[\text{Pb}(\text{L}^7)]^{2+}$, the lead(II) ion is bound to the eight available donor atoms of the bibracchial lariat ether as shown in Figure 1a, with distances $\text{Pb}-\text{O}(2)$ and $\text{Pb}-\text{O}(3)$ being, respectively, 0.09 and 0.04 Å longer than the sum of the van der Waals radius of oxygen and the ionic radius of lead(II), which amounts to 2.67 Å.^{27,28} In $[\text{Pb}(\text{L}^8-\text{H})]^+$, the lead(II) ion is directly bound to the phenolate oxygen atom, O(4); the nitrogen atom of the imine group, N(3); the nitrogen atom of the NH_2 group, N(4); the two bridgehead nitrogen atoms, N(1) and N(2); and one of the oxygen atoms of the crown moiety, O(1). Now, the remaining two $\text{Pb}-\text{O}$ distances ($\text{Pb}-\text{O}(2) = 3.077(13)$ Å and $\text{Pb}-\text{O}(3) = 3.008(15)$ Å) are clearly longer than the sum of the van der Waals radius of oxygen and the ionic radius of lead(II) by ca. 0.41 and 0.34 Å, respectively, and they can be regarded only as weak interactions. The question is whether this is due to an active

(24) (a) Platas-Iglesias, C.; Esteban, D.; Ojea, V.; Avecilla, F.; de Blas, A.; Rodríguez-Blas, T. *Inorg. Chem.* **2003**, *42*, 4299. (b) Gonzalez-Lorenzo, M.; Platas-Iglesias, C.; Avecilla, F.; Faulkner, S.; Pope, S. J. A.; de Blas, A.; Rodríguez-Blas, T. *Inorg. Chem.* **2005**, *44*, 4254.
 (25) Bashall, A.; McPartlin, M.; Murphy, B. P.; Powell, H. R.; Waikar, S. *J. Chem. Soc., Dalton Trans.* **1994**, 1972.
 (26) Platas, C.; Avecilla, F.; de Blas, A.; Rodríguez-Blas, T.; Bastida, R.; Macías, A.; Rodríguez, A.; Adams, H. *J. Chem. Soc., Dalton Trans.* **2001**, 1699.

(27) Ahrens, L. H. *Geochim. Cosmochim. Acta* **1952**, *2*, 155.

(28) Pauling, L. *The Nature of the Chemical Bond*, 3rd ed.; Cornell University Press: Ithaca, NY, 1960.

Table 3. Experimental (from X-ray diffraction) and Calculated (B3LYP/6-31G*) Bond Lengths (Å) of the Pb(II) Coordination Environment Obtained for the $[\text{Pb}(\text{L}^7)]^{2+}$ and $[\text{Pb}(\text{L}^8\text{-H})]^+$ Systems^a

$[\text{Pb}(\text{L}^7)]^{2+}$				
I		II		
	exp	calcd	calcd	
Pb–N(3)	2.781(6)	2.803	Pb–N(3)	3.863
Pb–O(1)	2.546(5)	2.632	Pb–O(1)	2.538
Pb–N(2)	2.650(6)	2.692	Pb–N(2)	2.864
Pb–N(4)	2.651(5)	2.669	Pb–N(4)	2.671
Pb–N(5)	2.668(6)	2.776	Pb–N(5)	2.880
Pb–N(1)	2.794(6)	2.833	Pb–N(1)	2.685
Pb–O(3)	2.712(7)	2.677	Pb–O(3)	2.669
Pb–O(2)	2.765(5)	2.815	Pb–O(2)	2.566
AF_i^b	0.021			

$[\text{Pb}(\text{L}^8\text{-H})]^+$				
I		II		
	calcd	exp	calcd	
Pb–O(4)	2.199	Pb–O(4)	2.273(11)	2.203
Pb–O(1)	3.000	Pb–O(1)	2.538(12)	2.574
Pb–N(3)	2.510	Pb–N(3)	2.621(11)	2.543
Pb–N(4)	2.761	Pb–N(4)	2.717(13)	2.781
Pb–N(2)	3.132	Pb–N(2)	2.752(13)	2.832
Pb–N(1)	2.929	Pb–N(1)	2.868(14)	3.008
Pb–O(3)	2.874	Pb–O(3)	3.008(15)	3.099
Pb–O(2)	2.719	Pb–O(2)	3.077(13)	3.222
AF_i^b			0.035	

^a See Figures 1–3 for numbering scheme. ^b Agreement factor between the experimental and calculated bond distances: $\text{AF}_i = [\sum(\text{exp} - \text{calcd})^2 / \sum(\text{exp})^2]^{1/2}$, where exp and calcd denote calculated and experimental values, respectively.

lone pair on the lead(II) atom or not. In the so-called hemidirected compounds, the lone pair of electrons can cause a nonspherical charge distribution around the Pb(II) cation; that is, the disposition of the ligands around the cation results in an identifiable void.⁵ While hemidirected compounds are rather easily identified for Pb(II) complexes with mono- or bidentate ligands, this is not the case for complexes with polydentate ligands such as L^8 . However, the presence of two long Pb–O distances in $[\text{Pb}(\text{L}^8\text{-H})]^+$, together with the rather spherical distribution of the donor atoms in $[\text{Pb}(\text{L}^7)]^{2+}$, suggests that the Pb(II) lone pair is stereochemically active in $[\text{Pb}(\text{L}^8\text{-H})]^+$. Further support for the stereochemical activity of the Pb(II) lone pair in $[\text{Pb}(\text{L}^8\text{-H})]^+$ comes from our DFT calculations described below. The angle formed between the planes of the benzyl and pyridine rings of the same pendant arm in $[\text{Pb}(\text{L}^7)]^{2+}$ amounts to 35.4°, whereas the angle between the planes of the benzyl and phenol rings of the same arm in $[\text{Pb}(\text{L}^8\text{-H})]^+$ is 43.1°. The presence of a pyridine or phenolate group in the ligand backbone appears to have an important effect on the dimensions of the cavity of the macrocyclic receptor in the complexes. Indeed, the distance between the two bridgehead nitrogen atoms is shorter in **1** ($\text{N}(1)\cdots\text{N}(5) = 4.929 \text{ \AA}$) than in **2** ($\text{N}(1)\cdots\text{N}(2) = 5.164 \text{ \AA}$). A similar situation happens when the distances between the imine nitrogen atom and the primary amine nitrogen atom are compared: $\text{N}(2)\cdots\text{N}(4) = 3.061 \text{ \AA}$ in **1** and $\text{N}(3)\cdots\text{N}(4) = 3.541 \text{ \AA}$ in **2**.

On the other side, the conformation that the macrocyclic receptor adopts in both complexes, $[\text{Pb}(\text{L}^7)]^{2+}$ and $[\text{Pb}(\text{L}^8\text{-H})]^+$, is significantly different. In the former, the pendant

arm containing the imine group is placed above the macrocyclic chain containing two ether oxygen atoms (Figure 1a), whereas in $[\text{Pb}(\text{L}^8\text{-H})]^+$, the arm containing the imine group is placed above the macrocyclic chain containing one oxygen atom (Figure 1b). Thus, complexes with ligands derived from 1,10-diaza-15-crown-5 containing two different pendant arms in syn orientation can adopt two different conformations depending on the position of the pendant arms over the macrocyclic fragment. In the following, we will refer to the conformation adopted by $[\text{Pb}(\text{L}^7)]^{2+}$ in the solid state as I, whereas the conformation that complex $[\text{Pb}(\text{L}^8\text{-H})]^+$ adopts in the solid state will be labeled as II. Figure 1 allows us to see how conformation II presents more steric hindrance than conformation I. Likewise, conformation I allows for maximization of the interaction of Pb(II) with the eight donor atoms of the macrocyclic receptor, whereas conformation II forces two oxygen atoms of the ligand (O(2) and O(3)) to be far from the metal ion, so that lower coordination numbers are obtained.

With the aim of understanding the reasons for these different conformations observed in the solid state for complexes $[\text{Pb}(\text{L}^7)]^{2+}$ and $[\text{Pb}(\text{L}^8\text{-H})]^+$, we have characterized both systems by means of DFT calculations (B3LYP model). For the two systems, both the I and II conformations were explored. In these calculations, the 6-31G* basis set was used for the ligand atoms. As there is not any all-electron basis set for lead, the effective core potential of Wadt and Hay (Los Alamos ECP) included in the LanL2DZ basis set was applied.^{16,17} Compared to an all-electron basis set, ECPs account for relativistic effects to some extent. It is believed that relativistic effects will become important for the elements from the fourth row of the periodic table. This ECP has been demonstrated to provide reliable results for different Pb(II) coordination compounds.^{29–31}

The calculated geometries of the I and II conformations of the $[\text{Pb}(\text{L}^7)]^{2+}$ system are shown in Figure 2, whereas calculated bond distances of the Pb(II) coordination environment are compared with experimental values in Table 3. The calculated structure corresponding to conformation I is quite similar to the solid-state X-ray one shown in Figure 1a. According to Table 3, the calculated bond lengths are in reasonably good agreement with those observed experimentally (within 0.11 Å), as evidenced by the excellent agreement factors obtained (Table 3, $\text{AF}_i = [\sum(\text{exp} - \text{calcd})^2 / \sum(\text{exp})^2]^{1/2}$, where exp and calcd denote experimental and calculated values, respectively).^{32,33} Calculated bond angles of the metal-coordination environment are also close to the experimental values (Table S2 of the Supporting Information). The calculated structure for conformation II shows the Pb(II) ion directly bound to seven of the eight available donor atoms of the ligand, because the nitrogen atom of the pyridine

(29) Yamaki, T.; Nobusada, K. *J. Phys. Chem. A* **2003**, *107*, 2351.

(30) Di Vaira, M.; Mani, F.; Constantini, S. S.; Stoppioni, P.; Vacca, A. *Eur. J. Inorg. Chem.* **2003**, 3185.

(31) Akibo-Betts, G.; Barran, P. E.; Puskar, L.; Duncombe, B.; Cox, H.; Stace, A. J. *J. Am. Chem. Soc.* **2002**, *124*, 9257.

(32) Willcott, M. R.; Lenkinski, R. E.; Davis, R. E. *J. Am. Chem. Soc.* **1972**, *94*, 1742.

(33) Davis, R. E.; Willcott, M. R. *J. Am. Chem. Soc.* **1972**, *94*, 1744.

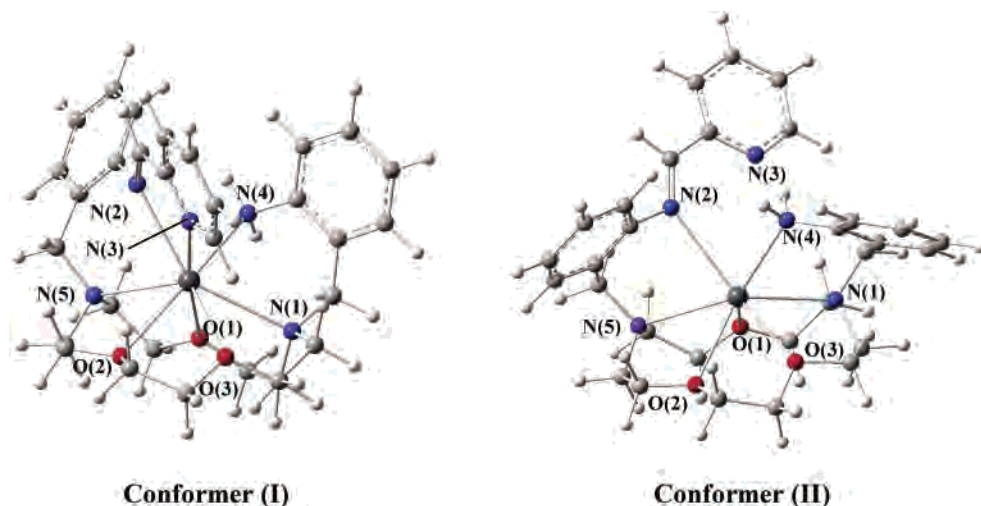


Figure 2. Structure of conformers I and II of $[\text{Pb}(\text{L}^7)]^{2+}$ as optimized in vacuo at the B3LYP/6-31G* level.

Table 4. Relative Energies (kcal mol^{-1}) of Conformers I and II. Calculated from DFT Calculations in Vacuo and in Acetonitrile Solution^a

	in vacuo		in solution ^b	
	6-31G*	6-31G*	6-31G*	6-311G**
$[\text{Pb}(\text{L}^7)]^{2+}$	8.99	10.49 ^c	10.05	
$[\text{Pb}(\text{L}^8\text{-H})]^+$	1.05	-1.30	-1.16	
$[\text{Pb}(\text{L}^8)]^{2+}$	6.96	6.67	6.26	
$[\text{Pb}(\text{L}^9\text{-H})]^+$	-3.50	-3.49	-3.38	
$[\text{Pb}(\text{L}^{10}\text{-H})]^+$	5.33	4.21	4.12	

^a The relative energy is defined as $E_{\text{rel}} = E_{\text{II}} - E_{\text{I}}$, and therefore a positive relative energy indicates that conformation I is more stable than conformation II. ^b Solvent effects have been included by using the COSMO model.

unit remains uncoordinated ($\text{Pb}-\text{N}(3) = 3.86 \text{ \AA}$). In parallel to the results from the X-ray studies, conformation I of $[\text{Pb}(\text{L}^7)]^{2+}$ was found by DFT to be that of lowest energy by ca. 9 kcal mol^{-1} . This is also true when solvent effects (acetonitrile) are taken into account (Table 4). The higher stability of conformation I compared to conformation II can be attributed to a more-favorable binding of the ligand donor atoms with Pb(II), with the metal ion being eight-coordinate in conformation I but only seven-coordinate in conformation II.

The calculated geometries of the I and II conformations of the $[\text{Pb}(\text{L}^8\text{-H})]^+$ system are shown in Figure 3, whereas calculated bond distances of the Pb(II) coordination environment are compared with experimental values in Table 3. The calculated conformation II is similar to the experimental X-ray structure. Most of the calculated Pb-donor bond distances are in good agreement with the experimental values (within 0.08 \AA), except the $\text{Pb}-\text{N}(1)$ and $\text{Pb}-\text{O}(2)$ distances, which deviate 0.12 and 0.14 \AA , respectively, from the experimental values. Calculated bond angles of the metal-coordination environment are also in reasonable agreement with the experimental values (Table S2 of the Supporting Information). On the other hand, the calculated geometry of $[\text{Pb}(\text{L}^8\text{-H})]^+$ corresponding to conformation I shows the Pb(II) ion being directly coordinated to the donor atoms of the pendant arms and to two oxygen atoms of the crown ether, whereas weaker interactions occur between the Pb(II) ion and both pivotal nitrogen atoms and one oxygen atom of

the crown moiety (Table 3). As contrasted with the X-ray evidence, our DFT calculations predict that conformation I is the most-stable one in vacuo by ca. 1 kcal mol^{-1} (Table 4). However, single-point energy calculations performed in acetonitrile solution (COSMO model) indicate that conformation II is the most-stable one in this solvent (Table 4). The use of a more-extended basis set for the ligand atoms (6-311G**) provides similar results (Table 4). A comparison of the relative energies of conformations I and II calculated for the $[\text{Pb}(\text{L}^7)]^{2+}$ and $[\text{Pb}(\text{L}^8\text{-H})]^+$ systems clearly shows that conformation II is more favored for the latter (Table 4).

DFT Studies: The Stereochemical Activity of the Pb(II) Lone Pair. Shimoni-Livny et al.⁵ have investigated a close relation between the role of a lone pair of Pb(II) and the coordination geometry for a number of Pb(II) complexes. They have found two general structural categories of Pb(II) compounds: holodirected and hemidirected, which are distinguished by the disposition of ligands around the metal ion. In the hemidirected form, there is a void in the liganding that is not found with holodirected geometry. These geometries can be interpreted using an orbital hybridization model; calculations indicate that in hemidirected Pb(II) complexes, there is both s and p character in the lead lone-pair orbital, whereas in holodirected complexes, only s character is observed.

An analysis of the natural bond orbitals (NBOs) in the conformations I and II of the $[\text{Pb}(\text{L}^7)]^{2+}$ entity shows that the Pb(II) lone-pair orbital remains almost entirely s in character: s[99.89%]p[0.11%] (I) and s[99.73%]p[0.27%] (II) (Table 5). This indicates that the $6s^2$ lone pair remains inactive, as expected for compounds with a rather spherical distribution of the donor atoms around the metal.

The analyses of the NBOs in $[\text{Pb}(\text{L}^8\text{-H})]^+$ shows that the Pb(II) lone pair orbital is still predominantly 6s, but polarized by some 6p contribution in both I and II conformations: s[98.80%]p[1.20%] (I) s[97.78%]p[2.22%] (II). Similar p contributions (1.89–4.39%) have been calculated for different hemidirected four-coordinate Pb(II) complexes with neutral ligands, whereas p contributions in the range 2.62–15.72% have been calculated for hemidirected four-

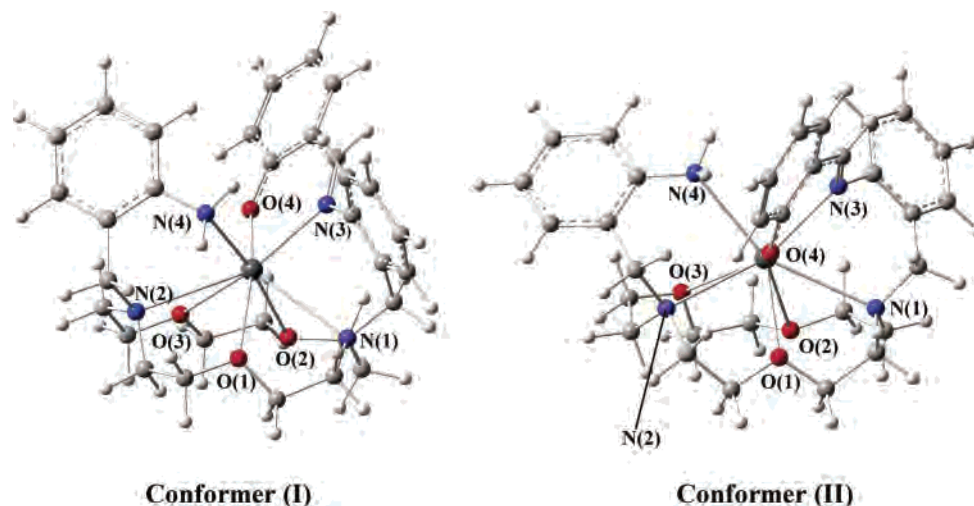


Figure 3. Structure of conformers I and II of $[\text{Pb}(\text{L}^8\text{-H})]^+$ as optimized in vacuo at the B3LYP/6-31G* level.

Table 5. Natural Bond Orbital (NBO) Analyses of the Pb(II) Lone Pair for Different Complexes

	conformation I	conformation II
$[\text{Pb}(\text{L}^7)]^{2+}$	s[99.89%]p0.00[0.11%]	s[99.73%]p0.00[0.27%]
$[\text{Pb}(\text{L}^8\text{-H})]^+$	s[98.80%]p0.01[1.20%]	s[97.78%]p0.02[2.22%]
$[\text{Pb}(\text{L}^8)]^{2+}$	s[99.84%]p0.00[0.16%]	s[99.66%]p0.00[0.34%]
$[\text{Pb}(\text{L}^9\text{-H})]^+$	s[99.26%]p0.01[0.74%]	s[98.22%]p0.01[1.78%]
$[\text{Pb}(\text{L}^{10}\text{-H})]^+$	s[99.12%]p0.01[0.88%]	s[98.25%]p0.01[1.75%]

coordinate Pb(II) complexes with anionic ligands.⁵ These results clearly confirm that the Pb(II) lone pair is stereochemically active in compound **2**, whereas in compound **1**, the Pb(II) lone pair remains inactive. Thus, the presence of a phenolate group instead of a pyridine unit in the ligand backbone appears to favor hemidirected geometries. The experimental Pb–O(4) bond distance in $[\text{Pb}(\text{L}^8\text{-H})]^+$ (2.271 Å, Table 3) is clearly shorter than the remaining Pb–N and Pb–O bond distances of the Pb(II) coordination sphere. This suggests that in complexes with polydentate ligands, hemidirected geometries may be favored by the presence of donor atoms with high affinity toward Pb(II). To confirm this hypothesis, we have performed DFT calculations on the $[\text{Pb}(\text{L}^8)]^{2+}$ system, where the phenol group is protonated, as well as in the related complexes $[\text{Pb}(\text{L}^9\text{-H})]^+$ and $[\text{Pb}(\text{L}^{10}\text{-H})]^+$, where $(\text{L}^9\text{-H})^-$ contains a thiophenolate group and $(\text{L}^{10}\text{-H})^-$ contains a pyrrolate unit. The corresponding calculated structures for both conformations are given in Figures 4–6, whereas the bond distances of the metal-coordination environment are reported in Table 6.

Upon protonation of the phenol group, the calculated distance between the Pb atom and the oxygen atom of the phenol group, O(4), increases by ca. 0.45 Å in both conformations (See Tables 3 and 6). In the two $[\text{Pb}(\text{L}^8)]^{2+}$ conformations, the lead ion is directly coordinated to the nine donor atoms of the ligand, with bond distances ranging from 2.58 to 2.95 Å (Table 6, Figure 4). This rather spherical distribution of the ligand donor atoms around the metal ion suggests that the Pb(II) lone pair remains inactive, and the geometries can be described as being holodirected. This is confirmed by the analysis of the NBOs (Table 5), which shows that upon protonation of the phenol group, the lead

Table 6. Bond Lengths (Å) of the Pb(II) Coordination Environment Calculated for the $[\text{Pb}(\text{L}^8)]^{2+}$, $[\text{Pb}(\text{L}^9\text{-H})]^+$, and $[\text{Pb}(\text{L}^{10}\text{-H})]^+$ Systems (B3LYP/6-31G* level)

	$[\text{Pb}(\text{L}^8)]^{2+}$		$[\text{Pb}(\text{L}^9\text{-H})]^+$		
	I	II	I	II	
Pb–O(4)	2.646	2.664	Pb–S(1)	2.701	2.689
Pb–O(1)	2.583	2.598	Pb–O(1)	2.969	2.591
Pb–N(3)	2.678	2.702	Pb–N(3)	2.571	2.639
Pb–N(4)	2.656	2.701	Pb–N(4)	2.737	2.795
Pb–N(2)	2.820	2.778	Pb–N(2)	3.031	2.890
Pb–N(1)	2.674	2.860	Pb–N(1)	2.957	2.910
Pb–O(3)	2.949	2.729	Pb–O(3)	2.841	3.105
Pb–O(2)	2.701	2.763	Pb–O(2)	2.798	3.185
	$[\text{Pb}(\text{L}^{10}\text{-H})]^+$				
	I		II		
Pb–N(3)	2.392		2.385		
Pb–O(1)	2.915		2.620		
Pb–N(2)	2.493		2.480		
Pb–N(4)	2.705		2.791		
Pb–N(5)	2.924		2.907		
Pb–N(1)	3.010		2.993		
Pb–O(3)	2.865		3.093		
Pb–O(2)	2.736		3.142		

lone pair loses most of the 6p contribution and remains almost entirely s in character: s[99.84%]p[0.16%] (I) and s[99.66%]p[0.34%] (II).

On the other hand, replacing the phenolate group in $[\text{Pb}(\text{L}^8\text{-H})]^+$ by a thiophenolate unit, $[\text{Pb}(\text{L}^9\text{-H})]^+$, results in a somewhat-lower polarization of the Pb 6s lone pair, as it follows from the NBOs analysis (Table 5): s[99.26%]p[0.74%] (I) s[98.22%]p[1.78%] (II). However, the calculated 6p contribution is still relatively important. Our DFT calculations indicate that conformation II is the most stable not only in vacuo but also in acetonitrile solution. Inspection of this geometry (Figure 5) and the bond distances given in Table 6 indicates that the geometry of this conformation is very similar to that observed for the related $[\text{Pb}(\text{L}^8\text{-H})]^+$ and may be described as hemidirected. The lead(II) ion is directly bound to the thiophenolate sulfur atom, S(1); the nitrogen atom of the imine group, N(3); the nitrogen atom of the NH_2 group, N(4); the two bridgehead nitrogen atoms, N(1) and N(2); and one of the oxygen atoms of the crown moiety, O(1). The remaining two Pb–O distances, Pb–O(2)

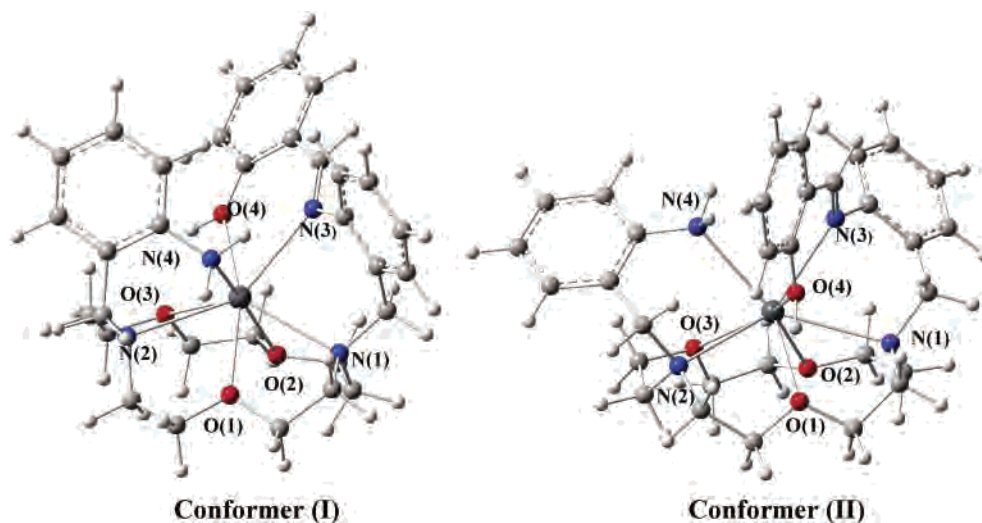


Figure 4. Structure of conformers I and II of $[\text{Pb}(\text{L}^8)]^{2+}$ as optimized in vacuo at the B3LYP/6-31G* level.

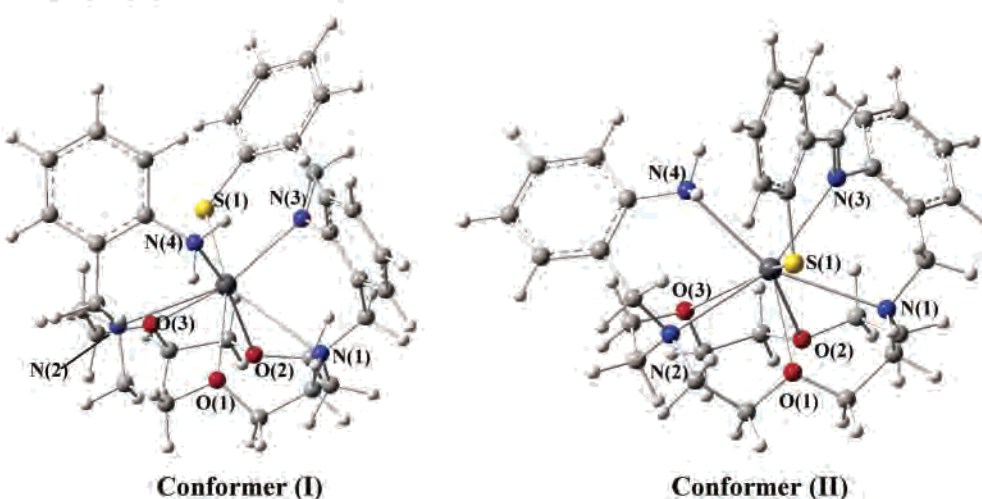


Figure 5. Structure of conformers I and II of $[\text{Pb}(\text{L}^9\text{-H})]^+$ as optimized in vacuo at the B3LYP/6-31G* level.

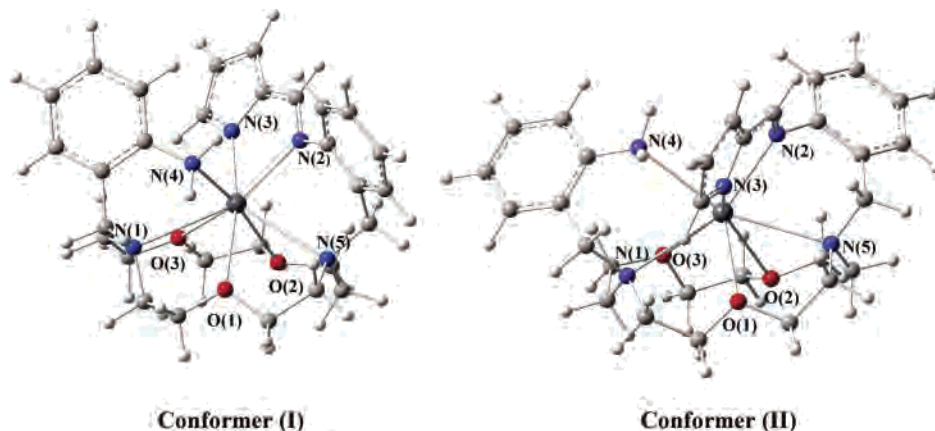


Figure 6. Structure of conformers I and II of $[\text{Pb}(\text{L}^{10}\text{-H})]^+$ as optimized in vacuo at the B3LYP/6-31G* level.

and Pb–O(3), are clearly longer than the sum of the van der Waals radius of oxygen and the ionic radius of lead(II); they can be regarded only as weak interactions. All these data suggest that the Pb(II) lone pair is stereochemically active in $[\text{Pb}(\text{L}^9\text{-H})]^+$, as it is in the analogous $[\text{Pb}(\text{L}^8\text{-H})]^+$. Finally, the data of the NBO analysis corresponding to $[\text{Pb}(\text{L}^{10}\text{-H})]^+$ (Figure 5) show that the replacement of a

pyridine group by a negatively charged pyrrolate unit results in a larger polarization of the lead 6s lone pair: s[99.12%]p[0.88%] (I) s[98.25%]p[1.75%] (II). Inspection of the data reported in Table 6 shows a more hemidirected geometry of $[\text{Pb}(\text{L}^{10}\text{-H})]^+$ in both conformations.

A comparison of the relative energies of conformations I and II calculated for the different complexes reported in this

work shows no direct correlation between the stabilization of conformation II and the polarization of the lead(II) lone pair. The results shown in Table 3 indicate that conformation II is more favored in those complexes with ligands containing phenol or thiophenol groups in the ligand backbone than in those with ligands containing pyridine or pyrrol units. In $[\text{Pb}(\text{L}^8\text{-H})]^+$ and $[\text{Pb}(\text{L}^9\text{-H})]^+$, the iminophenolate or iminothiophenolate units form six-membered chelate rings upon coordination to the metal ion, whereas in $[\text{Pb}(\text{L}^7)]^{2+}$ and $[\text{Pb}(\text{L}^{10}\text{-H})]^+$, the iminopyridine and iminopyrrolate units form five-membered chelate rings on coordinating to Pb(II). Therefore, the formation of six-membered chelate rings appears to stabilize conformation II with respect to conformation I. However, a comparison of the relative energies calculated for pairs of complexes with ligands of similar coordination properties in terms of the nature of the donor atoms and the size of the chelate rings formed by the coordination to the metal ion, ($[\text{Pb}(\text{L}^7)]^{2+}$ and $[\text{Pb}(\text{L}^{10}\text{-H})]^+$ or $[\text{Pb}(\text{L}^8)]^{2+}$ and $[\text{Pb}(\text{L}^8\text{-H})]^+$), shows that conformation II is stabilized on increasing the polarization of the lead(II) lone pair (see Tables 4 and 5).

The data presented here support the hypothesis that, in complexes containing high denticity ligands, hemidirected geometries might be favored by the presence of donor atoms with special greediness toward Pb(II). This means that not only the nature of the donor atom present in the polydentate ligand but also its charge has a main influence in the lead(II) lone-pair activity and, therefore, in the final geometry found in the corresponding lead(II) complex (hemi- or holodirected). In fact, our data show how a soft donor atom such as sulfur, which is usually found in lead(II) complexes with holodirected geometries, is able to force a hemidirected structure when it forms part of a anionic group and is incorporated into a polydentate backbone. Moreover, it has been asserted in the literature that for relatively electronegative donor atoms such as N or O, hemidirected structures were calculated to have more net positive charge on the Pb(II) ion than holodirected structures, and hence are energetically favored.⁶ However, our data have shown that, whereas $[\text{Pb}(\text{L}^8\text{-H})]^+$ presents a hemidirected geometry, as expected from the hard nature of the donors, in $[\text{Pb}(\text{L}^8)]^{2+}$, the lead lone pair is almost entirely s in character; so the lone pair remains inactive and the geometry can be described as being holodirected. Both L^8 and $(\text{L}^8\text{-H})^-$ are N_4O_4 octadentate ligands and have a similar degree of flexibility and the same topology; the main difference between them comes from their charge; L^8 is neutral, whereas $(\text{L}^8\text{-H})^-$ holds a negative charge.

Conclusions

Herein, we have studied the structural effect of the Pb(II) $6s^2$ lone pair in complexes with the unsymmetrical lariet ethers L^7 , L^8 , $(\text{L}^8\text{-H})^-$, $(\text{L}^9\text{-H})^-$, and $(\text{L}^{10}\text{-H})^-$. All these

ligands are octadentate, but they contain different aromatic units in their backbones: pyridine, phenol, phenolate, thiophenolate, and pyrrolate, respectively. In these lead(II) complexes, the receptor may adopt two possible conformations, depending on the disposition of the pendant arms over the crown moiety fragment: conformation I, in which the pendant arm holding the imine group is placed above the macrocyclic chain containing two ether oxygen atoms, and conformation II, in which such a pendant arm is placed above the macrocyclic chain containing the single oxygen atom. The X-ray crystal structures of compounds $[\text{Pb}(\text{L}^7)](\text{ClO}_4)_2$ (**1**) and $[\text{Pb}(\text{L}^8\text{-H})](\text{ClO}_4)$ (**2**) show that the former adopts conformation I, whereas $[\text{Pb}(\text{L}^8\text{-H})]^+$ adopts conformation II. Inspection of both crystal structures and metal–donor bond distances shows a holodirected geometry for $[\text{Pb}(\text{L}^7)]^{2+}$ and a hemidirected one for $[\text{Pb}(\text{L}^8\text{-H})]^+$, pointing so that the Pb(II) lone pair remains inactive in compound **1**, whereas in **2** the Pb(II) lone pair is stereochemically active. An analysis of the natural bond orbitals (NBOs) by using DFT calculations indicates that the Pb(II) lone-pair orbital remains almost entirely s in character in the $[\text{Pb}(\text{L}^7)]^{2+}$ complex, whereas in $[\text{Pb}(\text{L}^8\text{-H})]^+$, the Pb(II) lone pair is polarized by a certain 6p contribution, which confirms the stereochemical activity of the Pb(II) lone pair in the latter complex. Hemidirected geometries have been also found for $[\text{Pb}(\text{L}^9\text{-H})]^+$ and $[\text{Pb}(\text{L}^{10}\text{-H})]^+$, with ligands containing thiophenolate and pyrrolate groups, respectively. However, protonation of the phenolate group leads to a holodirected geometry, and the NBO analysis shows that now the lead lone pair remains almost entirely s in character.

All the data presented here support the hypothesis that, in complexes containing high denticity ligands, hemidirected geometries are favored by the presence of donor atoms with special greediness toward Pb(II), which means that not only the nature of the donor atom present in the polydentate ligand but also its charge has a main influence in the lead(II) lone-pair activity.

Acknowledgment. The authors thank Xunta de Galicia (PGIDIT03TAM10301PR) for generous financial support. The authors are indebted to Centro de Supercomputación of Galicia (CESGA) for providing the computer facilities.

Supporting Information Available: X-ray crystallographic files, in CIF format, for compounds **1** and **2**; Figure S1 showing ^1H NMR spectra of **1** and **2**; Table S1 listing calculated and experimental ^{13}C NMR shifts for **2**; Table S2 listing experimental and calculated angles of the metal coordination environments; and in vacuo optimized Cartesian coordinates (Å) for the $[\text{Pb}(\text{L}^7)]^{2+}$, $[\text{Pb}(\text{L}^8)]^{2+}$, $[\text{Pb}(\text{L}^8\text{-H})]^+$, $[\text{Pb}(\text{L}^9\text{-H})]^+$, and $[\text{Pb}(\text{L}^{10}\text{-H})]^+$ systems. This material is available free of charge via the Internet at <http://pubs.acs.org>.

IC060252M